Detection, Estimation & Tracking Road Objects for Assisting Driving

Afnan Alshkeili, Wenliang Qiu and Bidisha Ghosh
Dept. of Civil, Structural & Environmental Engineering, Trinity College Dublin, Ireland

Keywords: Multi-object Tracking, Object Detection, Traffic Flow Estimation, Distance Estimation.

Abstract: The new era of mobility is moving towards automation. Detecting, estimating, and tracking objects from moving vehicles using dash-cam images in real-time can provide substantial advantages in supporting drivers' decision making in advance. In this paper, an advanced deep learning-based object detection, distance estimation, and tracking framework has been proposed for this purpose. RetinaNet algorithm with ResNeXt backbone network has been used to detect five traffic object classes, including cars, cyclists, pedestrians, buses, and motorcycles, with improved accuracy. Additionally, distance estimation algorithm was introduced to increase both reliability and precession of detection. Moreover, an improved Simple Online and Real-time Tracking (SORT) algorithm were sequentially used to estimate traffic parameters such as volume and approach speed of each of these traffic object classes. The algorithm was trained and tested on stock imagery (COCO2017, MOT16, and TDD) of real-world videos taken from urban arterials with multimodal, signalized traffic operations.

1 INTRODUCTION

Autonomous vehicles (AV), self-driving cars, or driverless cars are widely used phrases to describe vehicles capable of sensing the environment and safely driving with no or little human inputs. These cars were introduced to reduce driving efforts, especially on urban roads (Aneesh et al., 2019), and due to their safety implications. It is estimated that the penetration rate of AV in traffic fleets can reduce traffic conflicts proportionally with over 90% reduction if all vehicles on the road are AVs (Papadoulis et al., 2019).

Concerning AVs, moving object detection, classification, and tracking algorithms have received extensive research attention. The object detection algorithms studied in literature considered multiple objects focusing primarily on pedestrians and road signs. R-CNN (Bunel et al., 2016) is a common deep learning algorithm used for object detection. However, this cannot be implemented for real-time on road traffic object detection due to high computational complexity. Faster R-CNN (Zhao et al., 2016) was developed to overcome this. The latest algorithms, such as Single Shot Multi-Box Detector (SSD) (Lin et al., 2017a) and You Only Look Once (YOLO) achieved high efficiency as they overcome some disadvantages presented in CNN and R-CNN. Gavrila (Gavrila, 2000) proposed a prototype system for pedestrian detection from a moving vehicle using a two-step approach algorithm. Lee et al. (Lee et al., 2009) developed an object detection algorithm in 3D cues for detecting pedestrians and vehicles. In 2013, (Felix Albu, 2013) invented an object detection from image profiles that is enables enhancing digital images.

In this paper, a RetinaNet based multi-class object detection and tracking framework is proposed to detect moving objects such as neighboring vehicles, pedestrians, and other traffic modes. By conducting vision-based analysis using video footage from a moving vehicle in an urban signalized road network. Detection based on RetinaNet has been investigated in the literature concerning autonomous driving. (Pei et al., 2020) (Aneesh et al., 2019)(Hoang et al., 2019) used a single-stage detector where RetinaNet was applied to form a traffic sign detection network and a CNN-based classifier for road signs, traffic light detection, and sign recognition. RetinaNet showed an improvement in detection accuracy and real-time classification operations. These algorithms have been used for multispectral pedestrian detection (Rajendran et al., 2019). Moreover, pedestrian detection has been investigated where (He and Zeng, 2017) has developed a warning system using Faster R-CNN that aims to lower traffic accidents.

Our proposed framework detected five different traffic-related objects (cars, buses, motorcycles, cyclists, and pedestrians) simultaneously using Reti-

Alshkeili, A., Qiu, W. and Ghosh, B.
Detection, Estimation Tracking Road Objects for Assisting Driving.
DOI: 10.5220/0010496806780685
In *Proceedings of the 7th International Conference on Vehicle Technology and Intelligent Transport Systems (VEHITS 2021)*, pages 678-685
ISBN: 978-989-758-513-5

naNet (Xie et al., 2017) having ResNeXt (Xie et al., 2017) as a backbone. The framework utilized a sequential tracking algorithm employing Simple Online and Real-time Tracking (SORT) to track all objects' classes. Furthermore, the framework estimated traffic parameters such as traffic volume, speed, and distance. Estimating these parameters using vision-based analysis from a moving vehicle by analyzing video images from a single camera source is a significant improvement in assisting driving. Results of the method were first trained on different datasets and then tested on single data.

The paper is organized as follows: Section 1 provides background and points on the associated topic's main algorithm. Section 2 covers the methodology used, and the framework developed. Section 3 highlights the data used for this paper. Section 4 an analysis and the results of the application. Finally, section 5 discusses the proposed method's applications, and a conclusion of the study is provided.

2 METHODOLOGY

The complete proposed framework for detecting moving objects from a moving vehicle in an urban transport network is described in this section.The theoretical background of the different elements of the framework is discussed.

The study focuses on developing methodologies for detecting, estimating, and tracking the flow, speed, and distance of pedestrians, cyclists, and other types of vehicles from an autonomous vehicle utilizing only visual information. The study utilizes videos captured from a single dash-cam of a human-driven car in the absence of access to an autonomous vehicle or appropriate video footage acquired from an autonomous vehicle.

2.1 Framework

The framework module consists of three main modules: detection, estimation, and tracking. The detection module consists of a RetinaNet detector, which contains the ResNeXt backbone network (Xie et al., 2017), Feature Pyramid Network (FPN) (Welch et al., 1995), and class/bbox subnets (Lin et al., 2017b) where it outputs a visual and a numerical results. The visual results are boundary boxes that show relative categories, and the numerical result is the confidence score, which is then fed to the next module. The estimation module, where the algorithm is adopted identifies the distance, volume, flow rate per second, and the detected pedestrian's speed. In this module, the only inputs that will be processed are pedestrians due to applying an object filter to select the pedestrian class from the detected results. It will output both visual and numerical results, a visual with distance indicated, and flow shown will be displayed and the estimated volume and flow will be displayed. The third module is the improved SORT tracking algorithm, which consists of Kalman prediction (Welch et al., 1995), object association, buffer module for miss detection, and tracking information update. The output result from the detection and estimation will be further tracked. Figure 1 provides schematics of the whole process.

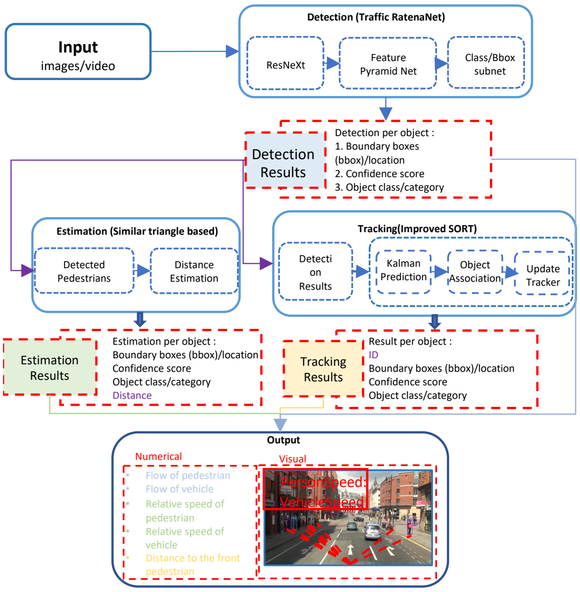

Figure 1: Framework of detection, tracking and estimation.

2.2 Traffic RetinaNet

This study uses a simple dense RetinaNet detector formed by improving existing single-stage object detection models presented in FPN for object detection and Focal Loss for Dense Object Detection . To initialize our network, we started by transfer learning using a pre-trained model. Thus we can use the weight and architecture obtain and apply it to our problem statement. ImageNet dataset is a widely used dataset to build various architectures since it is large enough to create a generalized model. The dataset is made of 14,197,122 images, 21841 synsets indexed, and about 500 images per node (Russakovsky et al., 2015a). The problem statement is to train a model to classify images into five different categories, as mentioned earlier. The pre-trained model shows a strong ability to generalize images outside the dataset (ImageNet) by transfer learning. Fine-tuning is the process in which model parameters are precisely adjusted to fit with certain observations (Gunawan et al., 2011). This was used on the COCO dataset in order for modifications to take place to suit our model.

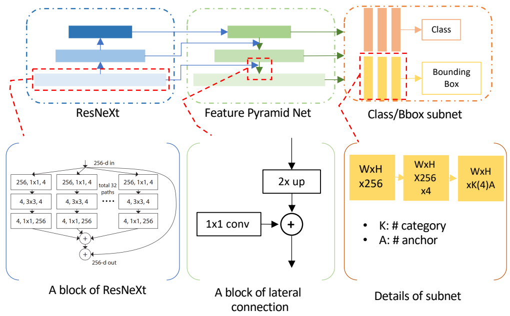

Figure 2: Framework of RetinaNet with ResNeXt backbone (Traffic RetinaNet).

2.2.1 ResNeXt

In order to achieve more efficient detection, we utilize ResNext (Xie et al., 2017) as the backbone of, as shown in Figure 2. The initialization product and fine-tuning output obtained from the previous steps are now feed into ResNeXt. The network is made of repeated building blocks that aggregates through several transformations with the same topology. ResNeXt is a homogeneous, multi-branch architecture that has only a few hyper-parameters to set. As shown in Figure 2, the input image passes through a set of lower-dimensional embeddings (by 1×1 convolutions), followed by specialized filters (3x3, 5×5, etc.). A block of ResNeXt with 32 cardinalities with similar complexity in which aggregation of residual transformation is performed (Xie et al., 2017). The output of each convolution is then passed to the feature pyramid net.

2.2.2 Feature Pyramid Net

Feature Pyramid Net (FPN) developed is an accurate in-network feature pyramid that can replace featured image pyramids without sacrificing representational power, speed, or memory (Lin et al., 2017a). This designed network passes the high-level semantic features to shallow layers using a lateral connection. In which each level of the pyramid is detecting objects at a different scale. Figure 2(top middle) illustrates the pathway, and Figure 2(bottom middle) shows the lateral connection details. The outputs are then passed to the last subnet.

2.2.3 Class/Box Subnet

For each pyramid level, a featured network attached to it. As shown in Figure 2(right), the classification subnet predicts the object's present probability at each position. The box regression subnet in Figure 2(bottom right) regresses each anchor's offset and matches it to the nearest ground-truth. Both subnets (object classification and box regression) though sharing a common structure, use separate parameters (Lin et al., 2017b).

2.2.4 Focal Loss

Focal Loss is an improvement on cross-entropy loss that reduces the relative loss for well-classified examples and focuses on challenging, misclassified examples (Lin et al., 2017b). Equations to calculate the cross-entropy losses were adopted from (Lin et al., 2017b) where:

$$FL(p,t) = -\alpha_t(1-p_t)^{\gamma}log(p_t) \qquad (1)$$

where α is the weighting factor and $(1-p)^{\gamma}$ is the modulating factor to the cross-entropy loss, with tunable focusing parameter $\gamma \geq 0$.

The proposed RetinaNet with ResNeXt backbone network is termed as Traffic-RetinaNet (TRN) from this section onwards. The output obtained from this algorithm (boundary box that illustrates the location of the object, configuration score, and the object class) used as an input for both estimation and tracking.

2.3 Distance Estimation

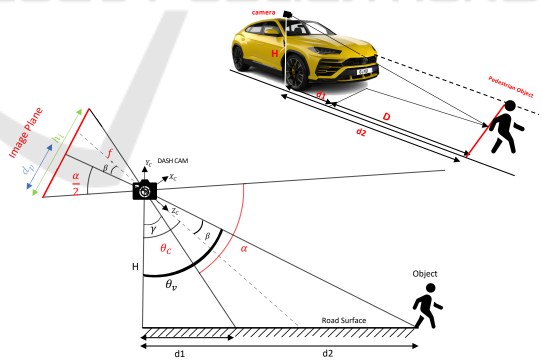

Figure 3: Distance estimation in 2D image plane.

After detection, a pedestrians object filter is applied, using a similar triangle-based distance estimation algorithm to estimate the distance of road objects more accurately. The center point of the bottom line of the boundary box is considered as the input for this stage.

We performed an experiment in which a dash-cam was located toward the car rear mirror looking forward at a height H above the road surface, and an angle α, the camera was tilted at an angle θ_c in $XcYcZc$ coordinates. Supposing the detected object on the road sense, located on an unknown position $(XwYwZw)$. θ_v is the angle of the projected ray (from the camera) pointing to the intersection of the planar of the detected object with the road surface planar, as shown in Figure 3 (the top figure). The distance D is the actual distance between the vehicle and the object that is equal to $d2 - d1$ can be calculated using the following equation (Rezaei et al., 2015):

$$\begin{aligned} D &= H * tan(\theta_v) - H * tan(\gamma) \\ &= H * \left[tan(\theta_c + \beta) - tan\left(\theta_c - \frac{\alpha}{2}\right)\right] \end{aligned} \quad (2)$$

To compute D we need β as both θ_c and α are known. On the other hand, we have (Rezaei et al., 2015):

$$tan(\beta) = \frac{\left(\frac{h_i}{2} - d_p\right)}{f} \quad (3)$$

where h_i is the hight captured image plane (in pixel), dp is the distance from the bottom side of the detected vehicle to the bottom of the image plane (in pixel), and f is the focal length of the camera. Where (Rezaei et al., 2015):

$$f = \frac{h_i}{2\tan\left(\frac{\alpha}{2}\right)} \quad (4)$$

Substituting all the parameters back to evaluate D we will get the following equation (Rezaei et al., 2015):

$$D = H * \left[\tan\left(\theta_c + \tan^{-1}\left(\frac{\frac{h_i}{2} - d_p}{\frac{h_i}{2\tan\left(\frac{\alpha}{2}\right)}}\right)\right) - \tan\left(\theta_c - \frac{\alpha}{2}\right)\right] \quad (5)$$

2.4 Improved Simple Online and Realtime Tracking (SORT)

Simple Online and Realtime Tracking (SORT) is a method used for online and real-time tracking. It tracks multiple objects in a simple, efficient manner. SORT algorithm combines both Kalman filter (Welch et al., 1995) and Hungarian (Kuhn, 1955) method thus to handle motion prediction and the data association components (Bewley et al., 2016).

Following both detection and estimation, tracking by detection using visuals only is introduced. The state of each detected object is modeled as:

$$x = [u, v, s, r, \dot{u}, \dot{v}, \dot{s}]^T \quad (6)$$

where u and v represent the targeted object's vertical pixel location. The other two variables, s, and r, correspond to scale (area) and the aspect ratio of the targeted object bounding box, respectively (Bewley et al., 2016).

The overlapping of objects in traffic scenes can result in miss tracking some of these objects. The original SORT algorithm failed to track those objects. To solve this issue, we proposed a simple yet powerful buffer module is introduced after the unmatched track-lets, as shown in Figure 4.

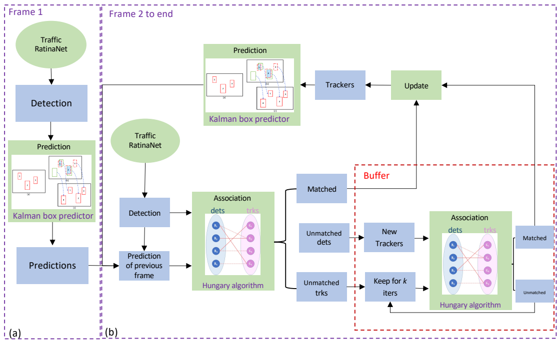

Figure 4: Framework of improved SORT.

2.5 Number and Speed Estimation

The number of objects in key classes and their approach speed are estimated based on the average difference of location in 5 consecutive frames. The flow was estimated and computed using the detection results (boundary box and class), where we considered only the detected objects of both cyclist and pedestrians class. Speed estimation carried out using tracking, where objects speed was estimated by computing the average difference of consecutive frames, as shown in the following equation (Kumar and Kushwaha, 2016):

$$S = \alpha \frac{1}{mn} \sum_{D} \sum_{n} df \quad (7)$$

where d is the difference in distance between consecutive frames in meter, f is the frame rate in frames/second, n is the number of tracking object (pedestrian / vehicle) per frame, m is the frame pair, and α is a parameter introduced to convert units to (meters/second).

3 DATASET

In this section, we will highlight the different datasets used for training and testing purpose. TRN was deployed on Ubuntu16.04 with pyTorch 1.2 environment. The backbone net was initialized according to ResNeXt (Hoang et al., 2019) pre-trained on ImageNet (Russakovsky et al., 2015b). The rest of conv layers except class/bbox subnet are initialized with bias, $b = 0$ and a Gaussian weight with standard deviation, $\sigma = 0.01$. For class/bbox subnet, the bias is initialized as $b = -\log_{10}((1-\tau)\tau)$, where $\tau = 0.01$. We trained the model with synchronized Stochastic Gradient Descent (SGD) over single GTX2080Ti GPUs with a total of 2 images per minibatch. The initial learning rate of 0.0025, weight decay of 0.0001 and momentum of 0.9 were used. Dataset was splited as follow 80000 images for training, 40000 for validation and 20000 for testing.

For estimation distance, we established a Traffic Distance Dataset (TDD) which was collected using dash camera, with 30 fps recording rate, a frame dimension of 1920 x 1080 pixel, 70° vertical field of view, camera was located at height $H = 155\ cm$ above road surface and tilled at an angle $\theta_c = 88.5°$. Those parameters where used to estimate distance using Matlab and to compare the obtained values to the ground truth values. Additionally, for testing purposes, different datasets (COCO data and data collected) are used to test pedestrians and cyclists' flow and volume.

We introduced an unsupervised learning method for tracking, where MOT (Multi-Object Tracking) dataset is used. We chose this particular dataset because it consists of the different classes we are interested in (pedestrians, vehicles, occlusion targets, and other categories). Improved SORT algorithm is then tested on the real-time data captured. Analysis and evaluation of all algorithms introduced and developed are evaluated and discussed in the next section.

4 ANALYSIS & RESULTS

4.1 Evaluation of TRN

4.1.1 Objective Evaluation of Detection using TRN

RetinaNet detector can work with different backbone encoders such as ResNet (He et al., 2016), ResNeXt (Hoang et al., 2019), and DenseNe (Lin et al., 2017b). Using ResNeXt as a backboned, we managed to increase the detection's average precision compared to the original RetinaNet, which includes a ResNet backbone (A.Alshkeili et al., 2019). Table 1 show the results obtained by applying the proposed algorithm on the COCO2017 dataset.

In this application, small stands for object had a pixel area of $< 32^2$ pixels. Medium stands for objects with an area range of $32^2 < area < 96^2$ pixels. Large stands for objects with an area of $96^2 < area$ pixels. The object detection results showed that both the AP and AR values improved for TRN except in medium objects. AP and AR were evaluated under IoU (Intersection over Union of boundary boxes) = 0.5 : 0.05 : 0.95 with AP: MaxDets = 100 (given 100 detection 100 image), AR: MaxDets = 1 (given 1 detection per image).

Table 1 shows the precision and recall for each category of objects detected. TRN achieves good results on pedestrians and buses, reasonable for cars and motorcycles but limited for cyclists. The main reason for this is the imbalance of training data in the COCO2017 dataset as it is not designed for this specific purpose of object detection from moving vehicles. However, due to the lack of an appropriately labeled dataset for evaluating these algorithms, it was prudent to use a well-known stock video such as COCO2017.

Table 1: Average percentage and average recall of the different categories.

Detected objects	Average Precision			
	All	Small	Medium	Large
Pedestrian	0.513	0.335	0.593	0.689
Cyclist	0.263	0.155	0.322	0.506
Car	0.393	0.301	0.549	0.563
Motorcycle	0.384	0.215	0.34	0.55
Bus	0.595	0.17	0.4	0.763
Detected objects	Average Recall			
	All	Small	Medium	Large
Pedestrian	0.185	0.475	0.685	0.776
Cyclist	0.223	0.268	0.5	0.0718
Car	0.172	0.459	0.687	0.756
Motorcycle	0.251	0.338	0.509	0.675
Bus	0.481	0.331	0.649	0.843

4.1.2 Subjective Evaluation of Detection using TRN

In Figure 5, a chosen set of scenes detecting all object types for illustrative purposes. The algorithm successfully detected different traffic object classes in the same scene, as shown in the images. TRN successfully classifies the different objects from different angles and distances, which is crucial for analyzing dash-cam footage from a moving vehicle where the angles and distance are uncontrollable. The objects were detected both in shadows and in illuminated areas of the same scene. Additionally, occlusion effects were minimized as a large number of bounding boxes (bbox) were identified in images in multiple objects.

4.1.3 Computational cost of Traffic RetinaNet

It is essential to estimate any traffic object-detection algorithms' computational costs to establish whether real-time detection is plausibility. Floating-point operation per second (FLOPs) is how fast the micropro-

Figure 5: Detection of multiple classes of objects in MOT16 dataset.

cessor operates; it has a performance unit of the multiplier–accumulator (Mac). Table 2 shows the performance parameters and FLOPs of the framework.

Table 2: Computational performance of the framework.

FLOPs:286.83 GigaMAC	Parameters: 54.86 Million	
	Training	Testing
Detection using TRN	3 days 18 h	9 Frames/Sec
Tracking	-	263 Frames/Sec

The detection is at the rate of 9 fps, which is slightly slower than a video rate of 30 fps. However, this rate can be considered real-time for vehicles and pedestrians in urban signalized roads from a relative movement point of view. The tracking rate is much higher than the video rate and is compatible with AV advanced collision avoidance alarm requirements.

4.2 Evaluation of Tracking

4.2.1 Objective Evaluation of Tracking

In traffic scenes, the object's scale is changing, so scale-insensitivity is crucial for the tracker. We chose SORT as it tracks objects only depending on the IoU region of objects, robust to object size. Table 3 shows the results of the improved SORT described earlier. The specific evaluation indicators used are (Welch et al., 1995):

- IDF1 : The ratio of correctly identified detections over the average number of ground-truth and computed detections
- IDP : Identification precision
- IDR : Identification recall
- GT : Total Number
- MT : Number of objects tracked for at least 80 percent of lifespan
- PT : Number of objects tracked between 20 and 80 percent of lifespan
- ML : Number of objects tracked less than 20 percent of lifespan.
- MOTA : Multiple object tracker accuracy.
- MOTP : Multiple object tracker precision.

Table 3: Comparing results of the original SORT to the improved.

	IDF1	IDP	IDR	GT	MT
SORT	44.1%	58.2%	35.5%	500	112
Imp	47.1%	56.9%	40.2%	500	118
	PT	ML	MOTA	MOTP	
SORT	224	164	32.9	73.7	
Imp	236	146	39.8	72.8	

Additionally, statistical estimation of the videos used presented in the following Table 4.

Table 4: Statistical Estimation Results of Videos.

Scene		(a)	(b)	(c)
Length (frames)		750	525	837
FPS		25	30	14
Av. Number	Ped.	14.7	14	8.7
	Veh.	9.8	0	0.7
Av. Speed	Ped.	3.48 m/s	1.7 m/s	1.87 m/s
	Veh	12.5 km/h	0 km/h	3 km/h

4.2.2 Subjective Evaluation of Tracking

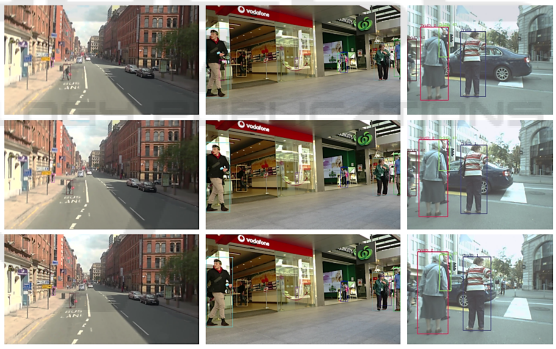

(a) (b) (c)

Figure 6: Tracking results in multiple scenes over three consecutive frames.

Figure 6 shows the result of tracking algorithm, where the distance and robustness of tracking vary between a) and c); thus, it shows the accuracy of the model.

Figure 7 illustrates the tracking of pedestrians for illustrative purposes; however, the framework was capable of tracking vehicles. The variables in the figure Q_p, Q_v, V_p and V_v (Q_p is the number of pedestrian,Q_v is the number of vehicles, V_p is the estimated pedestrian speed flow and V_v is the relative estimated speed flow of vehicle) shows the number of objects tracked and their average approach speed.

Figure 7: Flow and Speed estimation.

4.3 Distance, Speed and Flow Estimation

4.3.1 Objective Evaluation

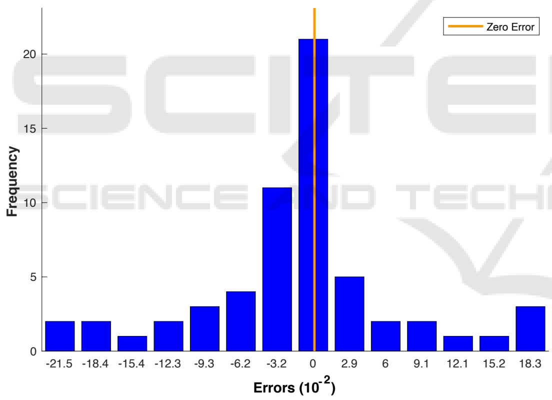

Figure 8: Percentage error of distance estimation.

Distance estimation error histogram illustrated in the following Figure 8 where the distance to vehicle errors, defined by comparing with ground truth represented by the red line. Objects are at a distance of 2 to 25m to the dash camera. We considered a confidence interval of $\pm 20cm$ for ground truth measurement. The error level lies between $\pm 20\%$, which is considered a reasonable percentage in our experiment.

4.3.2 Flow, Speed and Distance Evaluation

Figure 9 shows the flow of pedestrians and vehicles per frame. The curves' tendency illustrates the object speed Note that there is a gap around frame 480, as shown in blue curves; no vehicles exist in that period. Figure 10 presents an evaluation of the enter

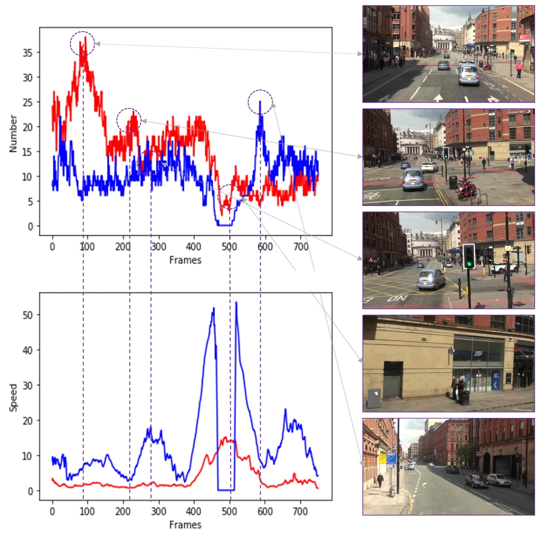

Figure 9: Number and Speed of Pedestrian and Vehicle in Scene (a).

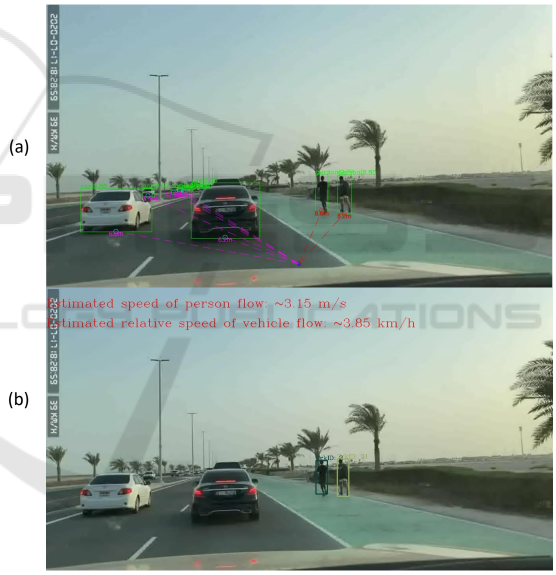

Figure 10: Detection, Tracking and estimation results.

algorithm applied to our data. (a) illustrates the detection and distance estimation results, (b) shows the both vehicle and pedestrian estimated flow.

5 DISCUSSION & CONCLUSION

This paper proposed a driver assistance framework based on visual information, including object detection, tracking, and traffic-related information estimation. Visual information is easier to obtain and applied to existing vehicles on a large scale than sensor information. Additionally, visual information is more in line with human perception of traffic. Based on the above considerations, this paper utilized the ResNeXt as the backbone net of the original RetinaNet, namely Traffic RetinaNet, thus enhancing object detection performance on five different traffic targets. Moreover, it also introduces the Improved SORT algorithm with a buffer module to enhance multi-object tracking's robustness. Finally, the object's category, trajectory, and location are used to inference the traffic flow, relative speed, and distance. The framework's performance succeeded in different light conditions, change of scenes due to the moving frame of reference, angles and relative distances, and crowded environments (occlusion). Comprehensive experiments and detailed analysis via visualization demonstrate the effectiveness of the proposed driver assistance framework.

REFERENCES

A.Alshkeili, Ghosh, B., and Qiu, W. (2019). Cyclist and pedestrian in autonomous vehicles view. In *Irish Transport Research Network (ITRN)*.

Aneesh, A. N., Shine, L., Pradeep, R., Moore, V. S., and Lopes, J. (2019). Real-time traffic light detection and recognition based on deep retinanet for self driving cars. In *2019 2nd International Conference on Intelligent Computing, Instrumentation and Control Technologies (ICICICT)*. ICICICT.

Bewley, A., Ge, Z., Ott, L., Ramos, F., and Upcroft, B. (2016). Simple online and realtime tracking. In *2016 IEEE International Conference on Image Processing (ICIP)*, pages 3464–3468.

Bunel, R., Davoine, F., and Philippe Xu (2016). Detection of pedestrians at far distance. In *2016 IEEE International Conference on Robotics and Automation (ICRA)*, pages 2326–2331.

Felix Albu, Larry Murray, P. S. I. R. (2013). Object detection from image profiles withinsequences of acouired digital images.

Gavrila, D. M. (2000). Pedestrian detection from a moving vehicle. In *European conference on computer vision*, pages 37–49. Springer.

Gunawan, A., Lau, H. C., and Lindawati (2011). Fine-tuning algorithm parameters using the design of experiments approach. In Coello, C. A. C., editor, *Learning and Intelligent Optimization*, pages 278–292, Berlin, Heidelberg. Springer Berlin Heidelberg.

He, K., Zhang, X., Ren, S., and Sun, J. (2016). Deep residual learning for image recognition. In *Proceedings of the IEEE conference on computer vision and pattern recognition*, pages 770–778.

He, X. and Zeng, D. (2017). Real-time pedestrian warning system on highway using deep learning methods. In *2017 International Symposium on Intelligent Signal Processing and Communication Systems (ISPACS)*, pages 701–706. IEEE.

Hoang, T. M., Nguyen, P. H., Truong, N. Q., Lee, Y. W., and Park, K. R. (2019). Deep retinanet-based detection and classification of road markings by visible light camera sensors. *Sensors*, 19(2):281.

Kuhn, H. W. (1955). The hungarian method for the assignment problem. *Naval research logistics quarterly*, 2(1-2):83–97.

Kumar, T. and Kushwaha, D. S. (2016). An efficient approach for detection and speed estimation of moving vehicles. *Procedia Computer Science*, 89(2016):726–731.

Lee, P., Chiu, T., Lin, Y., and Hung, Y. (2009). Real-time pedestrian and vehicle detection in video using 3d cues. In *2009 IEEE International Conference on Multimedia and Expo*, pages 614–617.

Lin, T.-Y., Dollár, P., Girshick, R., He, K., Hariharan, B., and Belongie, S. (2017a). Feature pyramid networks for object detection. In *Proceedings of the IEEE conference on computer vision and pattern recognition*, pages 2117–2125.

Lin, T.-Y., Goyal, P., Girshick, R., He, K., and Dollár, P. (2017b). Focal loss for dense object detection. In *Proceedings of the IEEE international conference on computer vision*, pages 2980–2988.

Papadoulis, A., Quddus, M., and Imprialou, M. (2019). Evaluating the safety impact of connected and autonomous vehicles on motorways. *Accident Analysis & Prevention*, 124:12–22.

Pei, D., Jing, M., Liu, H., Sun, F., and Jiang, L. (2020). A fast retinanet fusion framework for multi-spectral pedestrian detection. *Infrared Physics & Technology*, 105:103178.

Rajendran, S. P., Shine, L., Pradeep, R., and Vijayaraghavan, S. (2019). Fast and accurate traffic sign recognition for self driving cars using retinanet based detector. In *2019 International Conference on Communication and Electronics Systems (ICCES)*, pages 784–790.

Rezaei, M., Terauchi, M., and Klette, R. (2015). Robust vehicle detection and distance estimation under challenging lighting conditions. *IEEE Transactions on Intelligent Transportation Systems*, 16(5):2723–2743.

Russakovsky, O., Deng, J., Su, H., Krause, J., Satheesh, S., Ma, S., Huang, Z., Karpathy, A., Khosla, A., Bernstein, M., and et al. (2015a). Imagenet large scale visual recognition challenge. *International Journal of Computer Vision*, 115(3):211–252.

Russakovsky, O., Deng, J., Su, H., Krause, J., Satheesh, S., Ma, S., Huang, Z., Karpathy, A., Khosla, A., Bernstein, M., et al. (2015b). Imagenet large scale visual recognition challenge. *International journal of computer vision*, 115(3):211–252.

Welch, G., Bishop, G., et al. (1995). An introduction to the kalman filter.

Xie, S., Girshick, R., Dollár, P., Tu, Z., and He, K. (2017). Aggregated residual transformations for deep neural networks. In *2017 IEEE Conference on Computer Vision and Pattern Recognition (CVPR)*, pages 5987–5995.

Zhao, X., Li, W., Zhang, Y., Gulliver, T. A., Chang, S., and Feng, Z. (2016). A faster rcnn-based pedestrian detection system. In *2016 IEEE 84th Vehicular Technology Conference (VTC-Fall)*, pages 1–5.